Revision 2

Zhonghongite, Cu_{29} (As, Sb)$_{12}S_{33}$, a new mineral from the high-sulfidation vein of Jiama porphyry system, Tibet, China.

Shi-Ji Zheng[1*], Xiang-Ping Gu[2], Zhong-Jie Bai[1], Zhong-Kun Zhang[3]

[1] Institute of Geochemistry, Chinese Academy of Science, Guiyang, Guizhou 550081, China.

[2] School of Geosciences and Info-Physics, Central South University, Changsha, Hunan 410083, China.

[3] Tibet Huatailong Mining Development Co., Ltd, China National Gold Group, Lhasa 850200, China

*E-mail: zhengshiji@mail.gyig.ac.cn

ABSTRACT

Zhonghongite (IMA2023-046), ideally Cu_{29}(As, Sb)$_{12}S_{33}$, is a new mineral discovered in the high-sulfidation vein of the Jiama deposit (E 91°45', N 29°42'), southern Tibet, China. It forms complex intergrowths with watanabeite and tennantite-tetrahedrite, creating veined or massive aggregates ranging from millimeters to centimeters in size. The single crystals of zhonghongite are anhedral grains, with sizes ranging from several micrometers to approximately 100 micrometers. The mineral is gray in color with a black streak and metallic luster. It is brittle, with uneven fractures, and has a calculated density of 4.925g/cm^3. The average values of electron microprobe analyses (wt.%) are as follow: Cu 42.19, As 11.11, Sb 16.09, S 25.45, Hg 3.73, Mn 0.67, and Te 0.28. The empirical formula, based on 33 sulfur apfu, is $(Cu_{27.60}Hg_{0.77}Mn_{0.51}Fe_{0.07}Ag_{0.02})_{\Sigma 28.97}(As_{6.16}Sb_{5.49}Te_{0.09})\Sigma_{11.74}S_{33}$. In zhonghongite, the substitution of Sb for As is limited, with the atomic ratio of As/(As+Sb) ranging from 0.457 to 0.629. Hg, Mn, and Fe, together with minor Cu, are divalent and serve for charge balance. Zhonghongite is orthorhombic, space group *F*2*mm* (42), a = 10.37741(5) Å, b = 14.69821(9)

Å, c = 36.7645(2) Å and V = 5607.66(5) Å^3. The crystal structure has been solved and refined by single-crystal X-ray diffraction with a final $R1$ = 0.0235 for 27028 (2467 unique) reflections. It is composed of individual AsS_3 tripyramids and clustered tripyramids As_4S_7, CuS_4 tetrahedra and CuS_3 planar triangles, connected through corner S atoms in tetrahedral coordination and octahedral coordination with Cu and/or As. The structure is a derivative of tetrahedrite-type structure. Zhonghongite was formed under high-temperature conditions and is classified as an intermediate-sulfidation state mineral.

Keywords: New mineral, Zhonghongite, $Cu_{29}(As, Sb)_{12}S_{33}$, Jiama deposit

INTRODUCTION

Sulfosalts with Cu, As, Sb and S are most commonly found in hydrothermal mineral deposits, where they form a significant economic constituent of various ores (Marshall and Fairbridge 1999). Some sulfosalts serve as genetic indicators for the ore deposits. For instance, the enargite/luzonite-famatinite series (Cu_3AsS_4-Cu_3SbS_4) represents the high-sulfidation state, whereas tennantite-tetrahedrite indicates an intermediate-sulfidation state (Einaudi et al., 2003). Cu-sulfosalts often exhibit extensive solid solution due to the substitution between As and Sb (Moëlo et al. 2008). The experimental studies on Cu-As-S, Cu-Sb-S, and Cu-As-Sb-S have identified phases including enargite, luzonite-famatinite, sinnerite, skinnerite, tennantite-tetrahedrite, chalcostibite, watanabeite, and lautite (Maske and Skinner 1971; Skinner et al. 1972; Luce et al. 1977; Tesfaye and Taskinen 2010). Most of these Cu-sulfosalts have been discovered in the high-sulfidation veins of the Jiama mine in China (Zheng et al. 2021), and a

new mineral with an ideal formula of $Cu_{29}(As, Sb)_{12}S_{33}$ was revealed by microprobe analysis, which falls between tennantite-tetrahedrite and watanabeite. The new mineral has been named zhonghongite in honor of Prof. Hong Zhong (1971 − 2023) from the Institute of Geochemistry, Chinese Academy of Sciences (IGCAS) and approved by the IMA CNMNC (2023-046). Prof. Zhong dedicated all his life to the study of earth sciences and developed a strong reputation for high-quality research on ore deposit geochemistry. He made significant contributions to IGCAS over twenty years with his conscientiousness and selfless dedication.

The type material is deposited at the Geological Museum of China, No. 16, Yangrou Hutong, Xisi, Beijing 100031, PR China, catalogue number GMCTM2023002.

OCCURRENCE AND PARAGENESIS

The giant Jiama polymetallic deposit, is located at E 91°45', N 29°42', about 70 km east of Lhasa, Tibet. This deposit is part of the eastern Gangdese porphyry belt on the Tibetan Plateau and it comprises porphyry Cu-Mo mineralization, skarn Cu-polymetallic mineralization, and later high-sulfidation (or Cordilleran) veins (Tang et al. 2010; Lin et al. 2019; Zheng et al. 2021). The main sulfides in the porphyry mineralization are chalcopyrite and molybdenite. The skarn mineralization contains bornite, chalcopyrite, molybdenite, wittichenite, sphalerite, galena, pyrite, and pyrrhotite, with the associated skarn minerals being primarily andradite, diopside, and wollastonite. Zhonghongite was discovered in the high-sulfidation veins (Fig. 1a). These veins, ranging in width from a few centimeters to 50 centimeters, are widely distributed throughout the ore field. They mainly trend NE (20–40°) and dip steeply southeastward, forming later than (and cutting through) the porphyry and skarn mineralization. The ore from

these veins contains 30–90 vol.% Cu–As–Sb–S sulfosalts (Fig. 1b), including enargite, luzonite, sinnerite, tennantite-tetrahedrite, watanabeite and chalcostibite (Zheng et al. 2021). Zhonghongite forms complex intergrowths with watanabeite and tetrahedrite, creating veined or massive aggregates that are millimeters to centimeters in size. Under an optical microscope, it's challenging to distinguish among watanabeite, zhonghongite and tennantite–tetrahedrite due to their similar optical characteristics (Fig. 2a). However, the boundaries between watanabeite, zhonghongite and tennantite–tetrahedrite are discernible in back-scattered electron imaging (Fig. 2b – d). Zhonghongite occurs between wantanabeite and tetrahedrite.

PHYSICAL AND OPTICAL PROPERTIES

Zhonghongite is gray in color with a black streak and metallic luster. The Mohs hardness is estimated to be between 4 and 4.5. It is brittle without cleavage. The calculated density is 4.925 g/cm^3 on the basis of the empirical formula and unit-cell parameters refined from single-crystal XRD data. Polished thin sections were done using the Logitech PM5 lapping and polishing system in IGCAS. Under the optical microscope, in plane-polarized reflected light, zhonghongite shows a gray color with a greenish tint, and weak bireflectance from greenish gray to light green, ΔR = 0.9 % (589nm). It is weakly anisotropic with rotation tints varying from brownish-gray to bluish-gray in crossed-polarized light. Internal reflections were not observed. Reflectance values measured in air using the SiC standard with a Leica DM2500p microscope with a 20× objective and the full set of reflectance values is shown in Fig.3 and Table 1.

CHEMICAL COMPOSITION

Quantitative chemical analyses of zhonghongite were conducted in IGCAS, using the JXA-8530F Plus electron probe microanalyzer at 25 kV accelerating voltage, 10 nA beam current, and a 5 μm beam diameter. The analytical results (Table. 2, A1) yield the concentrations (wt.%) of Cu 41.44-43.1, As 9.30-13.80, Sb 13.13-18.09, S 25.02-25.84, Hg 2.54-4.67, and Mn 0.49-0.98, with minor Te 0.05-0.63, Ag < 0.14 and Fe < 0.33. The empirical formula on the basis of 33 S *apfu* is $(Cu_{27.60}Hg_{0.77}Mn_{0.51}Fe_{0.07}Ag_{0.02})_{\Sigma 28.97}(As_{6.16}Sb_{5.49}Te_{0.09})_{\Sigma 11.74}S_{33}$. The negative correlation between As and Sb for watanabeite, zhonghongite and tennantite-tetrahedrite is indicative of their mutual substitution (Fig. 4). The range of As-Sb variation for zhonghongite lies between watanabeite and tetrahedrite, with the atom ratio of As/(As+Sb) ranging from 0.457 to 0.629.

X-RAY CRYSTALLOGRAPHY AND STRUCTURE DETERMINATION

A single crystal of zhonghongite (about 20×10×10 μm in size) was extracted from the polished thin section using a focused ion beam (FIB) of the FEI Scios DualBeam system in IGCAS. The single-crystal X-ray diffraction study was carried out in Central South University, with a Rigaku XtaLAB Synergy diffractometer with Cu*K*α radiation at 50 kV and 1mA. The diffraction data are indexed on an orthorhombic unit cell with a = 10.37741(5) Å, b = 14.69821(9) Å, c = 36.7645(2) Å, V=5607.66(5) Å^3, and Z = 4. The crystal structure of zhonghongite was solved in space group *F2mm* (#42) and refined using SHELX (Sheldrick 2015a, 2015b) embedded in Olex2 (Dolomanov et al. 2009). The final anisotropic full-matrix least-squares refinement on F^2 was completed with R_1 = 0.0234 for 2446 independent

reflections ($I > 4\sigma I$), and the refinement statistics are listed in appendix Table A2. The structural formula of zhonghongite derived from refinement is $Cu_{27.02}Hg_{0.92}Mn_{0.62}As_{6.46}Sb_{5.54}Te_{0.05}S_{33}$. The XRD powder pattern of zhonghongite was obtained on a Rigaku XtaLAB Synergy diffractometer with Cu$K\alpha$ radiation at 50 kV and 1 mA in Gandolphi powder mode and the data are listed in Table 3. The refined unitcell parameters from the powder diffraction data using the program of Holland and Redfern (1996) are: a = 10.3776(5) Å, b = 14.6929(5) Å, c = 36.687(1) Å, V = 5593.9(3) Å^3, Z = 4. The strongest diffraction lines of zhonghongite are [d in Å (I%) (hkl)]: 3.481 (3) (2 2 6), 2.991 (100) (2 4 0), 2.590 (27) (0 4 10), 1.834 (58) (0 0 20), 1.566 (25) (2 8 10), 1.499 (4) (4 8 0) and 1.298 (3) (0 8 20), which are almost identical to tennantite, but different in subsidiary diffraction lines (Fig. 5).

The structure of zhonghongite is composed of 11 anion sites (S1-S11), 5 sites for As(Sb) in tripyramidal coordination, labelled as As1…As5 in the order of decreasing As occupancy, 4 sites for Cu in planar triangle coordination labelled as Cu1…Cu4, and 5 sites for Cu(Hg) in tetrahedral coordination labelled as Cu5…Cu9 (Table. A3). A refinement of the structure indicates that there are also 5 disordered sites of low occupancies, *i.e.* Te1 is adjacent to As1 and As2 sites, Mn1 close to Cu1 site, Cu2a and Mn2b are close to Cu2 site, and Hg4 close to Cu4 site, respectively occupied by Te^{4+}, Cu^{2+}, Mn^{2+} and Hg^{2+} with an occupancy of 0.02 to 0.09. All the sites, except the five disordered sites, are refined anisotropically. The atomic coordinates and displacement parameters are listed in Tables A3 and A4, and selected bond lengths and angles are presented in Table 4.

Among the five tripyramidal-coordinated As(Sb) sites (As1…As5) in zhonghongite, As1 and As2 are obviously dominated by As with As occupancies from 0.93 to 0.95 and As(Sb)-S bonding lengths from 2.222 Å to 2.345 Å (average 2.277 Å), but As3, As4 and As5 are dominated by Sb with Sb occupancies from 0.55 to 0.93 and Sb(As)-S bonding lengths from 2.357 Å to 2.489 Å (average 2.408 Å). It is noted that the As2 and As5 pyramids are clustered into a 4-member group (As_4S_7). The planar 3-coordinated site (Cu1…Cu4) with Cu-S bonding lengths from 2.244 Å to 2.263 Å (average 2.250 Å) are fully occupied by Cu and corner-connected to form six CuS_3 cluster surrounding S11. The 4-coordinated tetrahedral sites (Cu5…Cu9) with Cu-S bonding lengths from 2.310 Å to 2.380 Å (average 2.341 Å) may be incorporated with Hg with an occupancy of 0.01-0.17 in Cu9, Cu8 and less Cu7. In zhonghongite, individual AsS_3 tripyramids and clustered tripyramids As_4S_7, CuS_4 tetrahedra and CuS_3 planar triangles are connected through sharing corner S atoms to form a three-dimensional framework. There are two types of coordination for S in zhonghongite, 4-coordinated S site (S1…S10) and 6-coordinated S site(S11). The 6-coordinated S site(S11) is the common corner to connect six CuS_3 planar triangles. S1, S3 are the common corners for 2 CuS_4 tetrahedra and 2 AsS_3 tripyramids, S2 for 3 CuS_4 tetrahedra and 1 AsS_3 tripyramid, S4 to S10 for 2 CuS_4 tetrahedra, 1 AsS_3 tripyramid, and 1CuS_3 planar triangle. The disordered sites, Mn1, Cu2a, Mn2b and Hg4, partially occupied by Mn^{2+}, Cu^{2+} and Hg^{2+} with an occupancy from 0.02 to 0.09, serve as charge balance together with Hg^{2+} at the Cu7, Cu8, Cu9 sites.

DISCUSSION

Enargite is the earliest formed Cu-sulfosalt, followed by watanabeite and tennantite-tetrahedrite in the high-sulfidation vein (Zheng et al., 2021). Watanabeite replaces enargite, zhonghongite is replaced by tetrahedrite, and zhonghongite occurs between watanabeite and tetrahedrite (Fig. 2b – d). This suggests the mineral paragenetic sequence is enargite → watanabeite → zhonghongite → tennantite–tetrahedrite. Zhonghongite, watanabeite, and tennantite-tetrahedrite are closely intergrown and share the same major elements: Cu, As, Sb, and S. Zhonghongite and tennantite exhibit similar power X ray diffraction pattern (Fig. 5) and crystal structures (Table. 5). Their intergrown association and chemical compositions illustrate an evolution from As-rich watanabeite, through zhonghongite, to Sb-rich tetrahedrite (Fig. 2). The contents of Hg, Mn, Fe and Te in zhonghongite fall between those of watanabeite and tetrahedrite (Table. A1). Hg, Mn and Fe are commonly divalent, and Te in the form of Te^{4+} substitution for Sb^{3+} in tetrahedrite-group (Jonhnson et al. 1988; Biagioni et al. 2020). Thus, Hg, Mn and Fe in zhonghonggite should be also divalent and Te should be tetravalent. Additionally, up to 1.07 wt.% Pb is found in several analysis for zhonghongite, but it is below detection limit in watanabeite and tetrahedrite.

Structurally, zhonghongite and tennantite are similar, with the same types of polyhedra, AsS_3 tripyramid, CuS_4 tetrahedra and CuS_3 planar triangle. The S atoms in these two minerals all exhibit tetrahedral coordination and octahedral coordination, and the 6-coordinated site is the common corner for six planar CuS_3 triangles. Tennantite, which is cubic, also has approximately the same *a* (Table.5). Their identical *a* axis of the unit cell is due to their same distance between the two proximal 6-coordinated S. The 4-coodinated S combines 2 CuS_4

tetrahedra, 1 CuS_3 triangle and 1 AsS_3 tripyrimid in both minerals. However, zhonghongite has additional 4-coodinated S atoms to combine 1 - 2 AsS_3 pyramids and 2 - 3 CuS_4 tetrahedra. It is noted that the clustered pyramids (As_4S_7) occur in zhonghongite, but not in tennantite (Fig. 6, 7). Similar clusters also exist in sinnerite in the forms of (As_3S_7) and (As_5S_{11}) (Bindi et al. 2013). The Sb substitution for As would enlarge the As-S bond lengths in AsS_3 tripyramid. The cluster of AsS_3 pyramids may cause less distortion for the structure, which limits the substitution between As and Sb and results in their limit solid solution for zhonghongite, watanabeite and sinnerite. Overall, the arrangement of the polyhedra in these minerals causes their different structure and limit their change in the chemical composition.

As(Sb) occupies only one site in the tennantite-tetrahedrite series, and As-endmember tennantite($Cu_{12}As_4S_{13}$) and Sb-endmember tetrahedrite ($Cu_{12}Sb_4S_{13}$) are simply divided based on the predominant occupancy rule (50 % rule) (Nickel 1992). As(Sb) in the zhonghongite has five sites, with Sb dominant in the three sites. According to the dominance rule, the formula for zhonghongite should be $Cu_{29}As_4Sb_8S_{33}$(Sb>As). However, it is not consistent with the result of structural refinement and the chemical composition (As>Sb). The above rule only applies to complete solid solution series，but not appropriate to the partial solid solution series (Nickel 1992; Nickel and Grice 1998). Watanabeite ($Cu_4(Sb_{0.26}As_{0.74})_2S_5$-$Cu_4(Sb_{0.55}As_{0.609})_2S_5$) is the partial solid solution (Luce et al. 1977). The compositions of watanabeite embrace 50% mark and do not appear to extend to either end member. Only one name for watanabeite, and the approved formula is $Cu_4(As, Sb)_2S_5$ (Nickel, 1992; Shimizu et al. 1993). Similarly, zhonghongite is a partial solid solution series, with the atom ratio of As/(As+Sb) ranging from 0.457 to 0.629. Therefore, the formula $Cu_{33}(As, Sb)_{12}S_{33}$ is more suitable for zhonghongite.

199

200 **IMPLICATIONS**

201 Zhonghongite, a new phase in the Cu-As-Sb-S system, has been found to clarify the evolution
202 of Cu-As-Sb-S sulfosalts in the high-sulfidation vein of the Jiama mine. The paragenetic
203 sequence of Cu-As-Sb-S minerals indicates a transition from a high- to intermediate-sulfidation
204 state. Zhonghongite shares a similar structure or chemical composition with watanabeite and
205 tennantite-tetrahedrite and forms between them. Experimental studies have shown that
206 watanabeite and tennantite coexist under high-temperature conditions (350 − 500°C) (Luce et
207 al. 1977; Tesfaye and Taskinen 2010). In the natural ore deposits, massive Cu-As-Sb-S
208 assemblages are believed to be deposits derived from the Cu-sulfosalt melt, which are products
209 of condensation or rapid deposition from high-temperature (>350 °C) magmatic vapor
210 transporting metals and semimetals via fractures (Mavrogenes et al. 2010; Henley et al. 2012;
211 Zheng et al. 2021). Therefore, zhonghongite is expected to form under high-temperature
212 conditions and is one of the minerals indicating an intermediate-sulfidation state.
213 Cu-As-Sb-S sulfosalts are the primary constituents in high-sulfidation lode deposits, with gold
214 (Au) and silver (Ag) being the most economically valuable metals for recovery (Jannas et al.
215 1990, 1999; Bendezú and Fontboté 2009; Fontboté and Bendezú 2009; Zheng et al. 2021). Gold
216 and silver are more commonly found in the form of tellurides and are spatially and genetically
217 associated with Cu-As-Sb-S minerals (Bendezú and Fontboté 2009; Cooke et al. 2011;
218 Voudouris et al. 2011). Au-Ag tellurides appear to be closely related to the evolution of
219 watanabeite − zhonghongite − tetrahedrite (Fig. 2b, 2c) in the Jiama deposit, providing a good
220 opportunity to investigate the relationship between Au-Ag-Te and Cu-As-Sb-S minerals.

221

222

ACKNOWLEDGMENTS

Two anonymous reviewers, and associate editor Fabrizio Nestola are thanked for their constructive comments on the manuscript. This study was supported by the Second Tibetan Plateau Scientific Expedition and Research (STEP) (2019QZKK0806), National Key Research and Development Program of China(2018YFA0702605), and the Science Fund for Creative Research Groups of the National Natural Science Foundation of China (No. 42121003), National Natural Science Foundation of China (No. 42122024, 42072054). We acknowledge Xiang Li, Jianguo Li, Shaohua Dong and Yuanyun Wen for their valuable assistance with SEM, FIB and EPMA.

REFERENCES CITED

Bendezú, R., and Fontboté, L. (2009) Cordilleran epithermal Cu-Zn-Pb-(Au-Ag) mineralization in the Colquijirca district, central Peru: Deposit-scale mineralogical patterns. Economic Geology, 104, 905–944, https://doi.org/10.2113/econgeo.104.7.905.

Biagioni, C., George, L.L., Cook, N.J., Makovicky, E., Moëlo, Y., Pasero, M., Sejkora, J., Stanley, C.J., Welch, M.D., and Bosi, F. (2020) The tetrahedrite group: Nomenclature and classification. American Mineralogist: Journal of Earth and Planetary Materials, 105, 109–122, https://doi.org/10.2138/am-2020-7128.

Bindi, L., Makovicky, E., Nestola, F., and De Battisti, L. (2013) Sinnerite, $Cu_6As_4S_9$, from the Lengenbach quarry, Binn Valley, Switzerland: description and re-investigation of the crystal structure. The Canadian Mineralogist, 51, 851–860, https://doi.org/10.3749/canmin.51.6.851.

Cooke, D.R., Deyell, C.L., Waters, P.J., Gonzales, R.I., and Zaw, K. (2011) Evidence for magmatic-hydrothermal fluids and ore-forming processes in epithermal and porphyry deposits of the Baguio

district, Philippines. Economic Geology, 106, 1399–1424, https://doi.org/10.2113/econgeo.106.8.1399.

Dolomanov, O.V., Bourhis, L.J., Gildea, R.J., Howard, J. a. K., and Puschmann, H. (2009) OLEX2: a complete structure solution, refinement and analysis program. Journal of Applied Crystallography, 42, 339–341, https://doi.org/10.1107/S0021889808042726.

Einaudi, M.T., Hedenquist, J.W., and Inan, E.E. (2003) Sulfidation state of fluids in active and extinct hydrothermal systems: transitions from porphyry to epithermal environments. Special Publication-Society of Economic Geologists, 10, 285–314, https://doi.org/10.5382/SP.10.15.

Fontboté, L., and Bendezú, R. (2009) Cordilleran or Butte-type veins and replacement bodies as a deposit class in porphyry systems, pp. 521–523. Presented at the Proceedings of the 10th Biennial Society of Geology Applied to Ore Deposits Meeting.

Henley, R.W., Mavrogenes, J., and Tanner, D. (2012) Sulfosalt melts and heavy metal (As-Sb-Bi-Sn-Pb-Tl) fractionation during volcanic gas expansion: the El Indio (Chile) paleo-fumarole. Geofluids, 12, 199–215, https://doi.org/10.1111/j.1468-8123.2011.00357.x.

Holland, T.J.B, and Redfern, S.A.T. (1997) Unit cell refinement from powder diffraction data: the use of regression diagnostics. Mineralogical Magazine, 61: 65–77.

Ilinca, G. (2022) Charge distribution and bond valence sum analysis of sulfosalts – The ECoN21 computer program. Minerals, 12, 924, https://doi.org/10.3390/min12080924.

Jannas, R.R., Beane, R.E., Ahler, B.A., and Brosnahan, D.R. (1990) Gold and copper mineralization at the El Indio deposit, Chile. Journal of Geochemical Exploration, 36, 233–266, https://doi.org/10.1016/0375-6742(90)90057-H.

Jannas, R.R., Bowers, T.S., Petersen, U., and Beane, R.E. (1999) High-sulfidation deposit types in the El Indio district, Chile. Soc. Econ. Geol. Spec. Publ, 7, 219–266, https://doi.org/10.5382/SP.07.07.

Jonhnson, N.E., Craig, J.R., and Rrmsrror, J.D. (1988) Crystal chemistry of tetrahedrite. American Mineralogist, 73, 389–397.

Lin, B., Tang, J.X., Tang, P., Zheng, W.B., Greg, H., Chen, G.L., and Zhang, Z.K. (2019) Polycentric complex mineralization model of porphyry system: A case study of Jiama superlarge deposit in Tibet. Mineral Deposits, 38, 1204–1222.

Luce, F.D., Tuttle, C.L., and Skinner, B.J. (1977) Studies of sulfosalts of copper: V, Phases and phase relations in the system Cu-Sb-As-S between 350°C and 500°C. Economic Geology, 72, 271–289, https://doi.org/10.2113/gsecongeo.72.2.271.

Marshall, C.P., and Fairbridge, R.W. (1999) Encyclopedia of geochemistry. Springer Science & Business Media.

Maske, S., and Skinner, B.J. (1971) Studies of the sulfosalts of copper: I, Phases and phase relations in the system Cu-As-S. Economic Geology, 66, 901–918, https://doi.org/10.2113/gsecongeo.66.6.901.

Mavrogenes, J., Henley, R.W., Reyes, A.G., and Berger, B. (2010) Sulfosalt melts: Evidence of high-temperature vapor transport of metals in the formation of high-sulfidation lode gold deposits. Economic Geology, 105, 257–262, https://doi.org/10.2113/gsecongeo.105.2.257.

Moëlo, Y., Makovicky, E., Mozgova, N.N., Jambor, J.L., Cook, N., Pring, A., Paar, W., Nickel, E.H., Graeser, S., and Karup-Møller, S. (2008) Sulfosalt systematics: a review. Report of the sulfosalt sub-committee of the IMA Commission on Ore Mineralogy. European Journal of Mineralogy, 20, 7–46, https://doi.org/10.1127/0935-1221/2008/0020-1778.

Momma, K., and Izumi, F. (2011) VESTA 3 for three-dimensional visualization of crystal, volumetric and morphology data. Journal of Applied Crystallography, 44, 1272–1276, https://doi.org/10.1107/S0021889811038970.

290 Nickel, E.H. (1992) Solid solutions in mineral nomenclature. Mineralogy and Petrology, 46, 49–53,
291 https://doi.org/10.1007/BF01160701.
292 Nickel, E.H., and Grice, J.D. (1998) The IMA Commission on New Minerals and Mineral Names: procedures
293 and guidelines on mineral nomenclature, 1998. Mineralogy and Petrology, 64, 237–263,
294 https://doi.org/10.1007/BF01226571.
295 Sheldrick, G.M. (2015a) Crystal structure refinement with SHELXL. Acta Crystallographica Section C:
296 Structural Chemistry, 71, 3–8, https://doi.org/10.1107/S2053229614024218.
297 ——— (2015b) SHELXT - Integrated space-group and crystal-structure determination. ACTA
298 Crystallographica Section A: Foundation and Advances, 71, 3–8,
299 https://doi.org/10.1107/S2053273314026370.
300 Skinner, B.J., Luce, F.D., and Makovicky, E. (1972) Studies of the sulfosalts of copper III: phases and phase
301 relations in the system Cu-Sb-S. Economic Geology, 67, 924–938,
302 https://doi.org/10.2113/gsecongeo.67.7.924.
303 Tang, J.-X., Wang, D.-H., Wang, X.-W., Zhong, K.-H., Ying, L.-J., Zheng, W.-B., Li, F.-J., Guo, N., and Qin,
304 Z.-P. (2010) Geological features and metallogenic model of the Jiama copper-polymetallic deposit in
305 Tibet. Diqiu Xuebao (Acta Geoscientica Sinica), 31, 495–506.
306 Tesfaye, F., and Taskinen, P. (2010) Thernmodynamics and Phase Equilibria in the (Ni, Cu, Zn)-(As, Sb, Bi)-
307 S Systems at Elevated Temperature (300 – 900°C).
308 Voudouris, P.C., Melfos, V., Spry, P.G., Moritz, R., Papavassiliou, C., and Falalakis, G. (2011) Mineralogy
309 and geochemical environment of formation of the Perama Hill high-sulfidation epithermal Au-Ag-Te-
310 Se deposit, Petrota Graben, NE Greece. Mineralogy & Petrology, 103, 79–100,
311 https://doi.org/10.1007/s00710-011-0160-z.

312 Zheng, S.-J., Zhong, H., Bai, Z.-J., Zhang, Z.-K., and Wu, C.-Q. (2021) High-sulfidation veins in the Jiama
313 porphyry system, South Tibet. Mineralium Deposita, 1–10, https://doi.org/10.1007/s00126-020-00955-
314 z.

315

316 **Figure captions**

317 **Figure 1.** The geological occurrence for zhonghongite. **(a)** the high-sulfidation vein controlled
318 by fracture, cutting skarn and hornfel; **(b)** the Cu-As-Sb-S ore containing zhonghongite from
319 the high-sulfidation vein.

320

321 **Figure 2.** Reflected-light photomicrograph (a) and back scattered electron (BSE) images (b -
322 d) for zhonghongite. **(a)** Light green zhonghongite has similar reflecting color to watanabeite.
323 **(b - d)** Zhonghongite occurs between watanabeite and tetrahedrite and their boundary are
324 clear. Enr: enargite; Wa: watanabeite; Zhh: zhonghongite; Td: tedrahedrite; Au-Ag-Tel: Au-
325 Ag tellurides.

326 **Figure 3.** Reflectance curves for zhonghongite in air.

327 **Figure 4. (a)** The ternary diagram for Cu-As(Sb)-S phases and the location for tennantite-
328 tetrahedrite, zhonghongite and watanabeite; **(b)** The variation range of As and Sb contents for
329 intergrown watanabeite, zhonghongite and tetrahedrite. Enr/luz-Fmt: enargite/luzonite-
330 famatinite, Tn-Td: tennantite-tetrahedrite, Sin: sinnerite, Wa: watanabeite, Ski: skinneite, Zhh:
331 zhonghongite, Chst: chalcostibite, Lt: lautite.

332

333 **Figure 5.** Calculated patterns of X-ray powder diffraction for zhonghongite and tennantite-(Zn).

334

335 **Figure 6.** The crystal structure of zhonghongite viewed along the c-axis plotted with VESTA
336 (Momma and Izumi 2011), showing the distribution and connectivity of Cu tetrahedra, Cu
337 planar triangles and As(Sb) tripyramids, and the locations of 6-coordinated S11 and disordered
338 Te1, Mn1, Cu2b.

339

340 **Figure 7.** Comparison of crystal structure between zhonghongite (a and b) and tennantite-(Zn)

(c and d) showing the arrangements of As(Sb) tripyramids (a and c) and the arrangements of CuS_4 tetrahedra and planar CuS_3 triangles (b and d). The legends are the same as Fig. 5.

Table 1. Reflectance data for zhonghongite

λ (nm)	R1	R2	λ (nm)	R1	R2
400	28.1	29.9	560	30.1	31.0
420	29.3	30.6	580	29.8	30.7
440	30.1	31.2	589 (COM)	29.6	30.5
460	30.6	31.5	600	29.4	30.3
470 (COM)	30.8	31.6	620	29.1	30.0
480	30.9	31.7	640	28.9	29.7
500	30.9	31.6	650 (COM)	28.9	29.6
520	30.8	31.5	660	28.9	29.5
540	30.5	31.3	680	29.1	29.4
546 (COM)	30.4	31.2	700	29.6	29.5

Table 2. Summary chemical data (wt. %) for zhonghongite

Element	Mean	Range	Stand. Dev. (σ)	*Apfu*	Reference Material
Cu	42.19	41.44--43.13	0.38	27.60	$CuFeS_2$
As	11.11	9.30--13.80	0.81	6.16	FeAsS
Sb	16.09	13.13--18.09	1.03	5.49	Sb_2S_3
S	25.45	25.02--25.84	0.19	33	$CuFeS_2$
Hg	3.73	2.54--4.67	0.49	0.77	HgS
Mn	0.67	0.49--0.98	0.12	0.51	Mn
Te	0.27	--0.63	0.13	0.09	Te
Ag	0.03	--0.14	0.04	0.02	Ag
Fe	0.09	--0.33	0.09	0.07	$CuFeS_2$
Pb	0.09	--1.07	0.26	0.02	PbS
Total	99.79	99.06--100.63	0.43		

This is the peer-reviewed, final accepted version for American Mineralogist, published by the Mineralogical Society of America.
The published version is subject to change. Cite as Authors (Year) Title. American Mineralogist, in press.
DOI: https://doi.org/10.2138/am-2024-9338. http://www.minsocam.org/

Table 3. X-ray powder diffraction data for zhonghongite

h k l	I_{cal}	I_{meas}	d_{cal}	d_{meas}	***h k l***	I_{cal}	I_{meas}	d_{cal}	d_{meas}
2 0 0	0.5	1	5.189	5.184	3 3 11	1.0	1	2.156	2.161
0 2 6	0.3	1	4.700	4.689	4 4 0	0.5	1	2.119	2.122
1 3 1	1.7	2	4.397	4.410	1 7 1	0.6	1	2.054	2.055
1 3 3	1.6	1	4.164	4.160	1 7 3	0.9	2	2.029	2.030
2 0 6	2.2	2	3.956	3.952	4 4 6	1.4	1	2.002	1.997
2 2 4	0.8	1	3.847	3.850	1 3 17	1.8	1	1.940	1.944
0 0 10	1.2	2	3.669	3.661	5 3 1	1.7	2	1.908	1.911
2 2 6	**2.5**	**3**	**3.483**	**3.481**	2 6 10	1.7	2	1.896	1.893
3 1 1	1.0	1	3.353	3.353	**0 0 20**	**13.3**	**58**	**1.834**	**1.834**
2 2 8	0.7	1	3.113	3.115	0 2 20	0.1	1	1.780	1.784
2 4 0	**100.0**	**100**	**2.998**	**2.991**	1 7 11	0.9	0	1.751	1.748
3 1 7	1.2	1	2.833	2.836	1 5 17	1.8	1	1.715	1.717
2 2 10	1.3	1	2.774	2.762	6 2 0	0.9	0	1.684	1.685
1 1 13	1.4	1	2.678	2.681	1 7 13	1.8	1	1.662	1.665
0 4 10	**25.3**	**27**	**2.596**	**2.590**	2 6 16	0.7	0	1.593	1.594
1 5 7	1.7	2	2.488	2.493	**2 8 10**	**15.2**	**25**	**1.566**	**1.566**
4 2 0	1.0	0	2.446	2.439	**4 8 0**	**2.7**	**4**	**1.499**	**1.499**
1 3 13	1.8	2	2.380	2.386	0 10 0	0.2	1	1.469	1.468
3 3 9	1.6	1	2.322	2.315	3 9 9	0.2	1	1.388	1.388
0 0 16	1.3	1	2.293	2.278	**0 8 20**	**5.0**	**3**	**1.298**	**1.298**
3 5 1	0.5	1	2.235	2.241					

Table 4. Selected bond distances and angles of zhonghongite.

For AsS_3 pyramids		For CuS_3 triangles	
As1—S4$^{\times 2}$	2.251(2) Å	Cu1—S5	2.253(4) Å
—S5$^{\times 1}$	2.248(3) Å	—S8	2.244(4) Å
Mean	2.250 Å	—S11	2.245(5) Å
As2—S3$^{\times 2}$	2.345(2) Å	Mean	2.247 Å
—S2$^{\times 1}$	2.222(3 Å	Cu2—S9	2.254(3) Å
Mean	2.304 Å	—S10	2.247(3) Å
As3—S6	2.357(2) Å	—S11	2.247(3) Å
—S7	2.367(2) Å	Mean	2.249 Å
—S9	2.367(2) Å	Cu3—S4	2.263(3) Å
Mean	2.364 Å	—S6	2.239(3) Å
As4—S8	2.378(3) Å	—S11	2.256(3) Å
—S10$^{\times 2}$	2.374(2) Å	Mean	2.253 Å
Mean	2.375 Å	Cu4—S7$^{\times 2}$	2.248(3) Å
As5—S1	2.480(3) Å	—S11	2.250(5) Å
—S3$^{\times 2}$	2.489(2) Å	Mean	2.249 Å
Mean	2.486 Å		
For CuS_4 tetrahedra		For CuS_4 tetrahedra	
Cu5—S1	2.412(4) Å	Cu6—S3	2.376(3) Å
—S2	2.325(3) Å	—S5	2.314(2) Å
—S4$^{\times 2}$	2.290(2) Å	—S6	2.326(3) Å
Mean	2.329 Å	—S7	2.312(3) Å
Cu7—S2	2.310(2) Å	Mean	2.332 Å
—S3	2.353(3) Å	Cu8—S7	2.385(3) Å
—S4	2.302(3) Å	—S8	2.361(3) Å
—S6	2.323(2) Å	—S9	2.356(2) Å
Mean	2.322 Å	—S10	2.366(3) Å
Cu9—S9$^{\times 2}$	2.380(2) Å	Mean	2.367 Å
—S10$^{\times 2}$	2.370(3) Å		
Mean	2.375 Å		
S4—As1—S5	101.34(6)°	S4—As1—S4	100.20(11)°
S2—As2—S3	97.37(7)°	S3—As2—S3	101.66(11)°
S6—As3—S7	97.59(7)°	S6—As3—S9	96.38(7)°
S8—As4—S10	96.14(7)°	S10—As4—S10	96.14(7)°
S1—As5—S3	98.50(7)°	S3—As5—S3	103.22(9)°
S5—Cu1—S8	97.70(15)°	S5—Cu1—S11	129.85(14)°
S9—Cu2—S10	97.94(10)°	S9—Cu2—S11	129.55(12)°
S4—Cu3—S6	101.62(10)°	S4—Cu3—S11	127.82(11)°
S7—Cu4—S7	98.37(16)°	S7—Cu4—S11	130.35(8)°

Table 5. Comparative characteristics of zhonghongite with tennantite.

	zhonghongite*	tennantite-(Zn)*
Empirical chemical formula from refinement	$Cu_{27.02}Hg_{0.92}Mn_{0.62}As_{6.47}Sb_{5.53}Te_{0.05}S_{33}$	$Cu_{10.00}Zn_{1.76}Hg_{0.24}(As_{3.22}Sb_{0.78})S_{13}$
Space group	*F*2*mm*	$I\bar{4}3m$
a(Å)	10.37741(5)	10.3270(15)
b(Å)	14.69821(9)	
c(Å)	36.7645(2)	
V(Å^3)	5607.66(5)	1101.3(3)
As—S in AsS_3 (Å)	2.277	2.315
Sb—S in SbS_3 (Å)	2.431	
Cu—S in CuS_3 (Å)	2.250	2.248
Cu—S in CuS_4 (Å)	2.341	2.353

Notes: * this study, samples from the Jiama Cu-polymetallic deposit, Tibet, China.

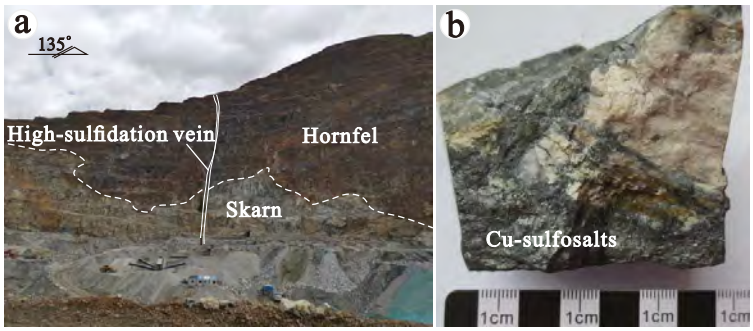

Fig.1

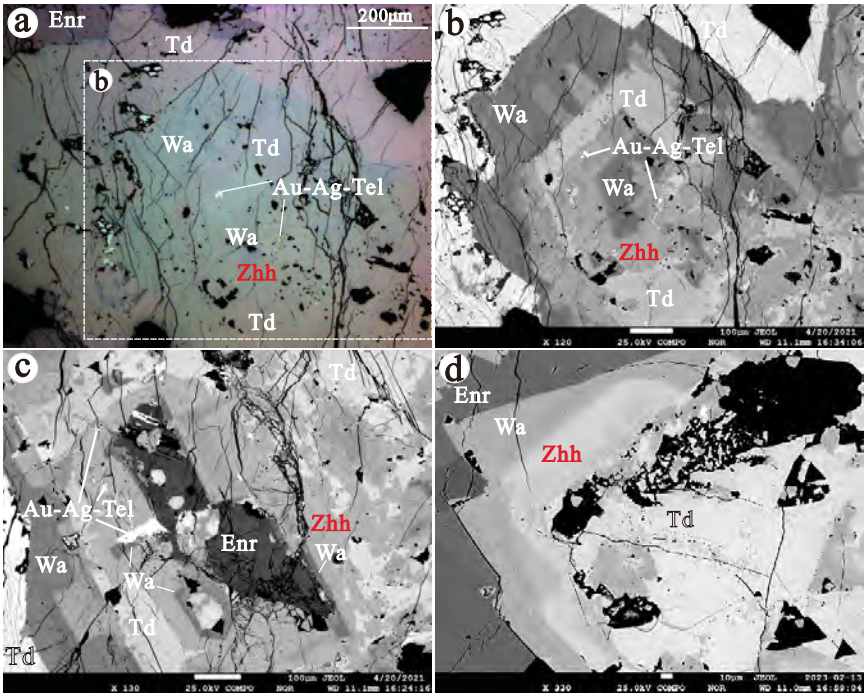

Fig.2

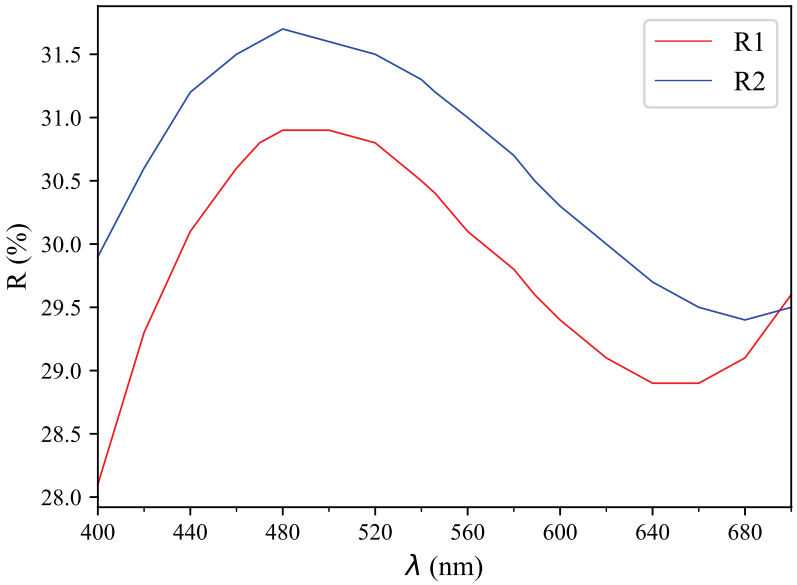

Fig.3

This is the peer-reviewed, final accepted version for American Mineralogist, published by the Mineralogical Society of America.
The published version is subject to change. Cite as Authors (Year) Title. American Mineralogist, in press.
DOI: https://doi.org/10.2138/am-2024-9338. http://www.minsocam.org/

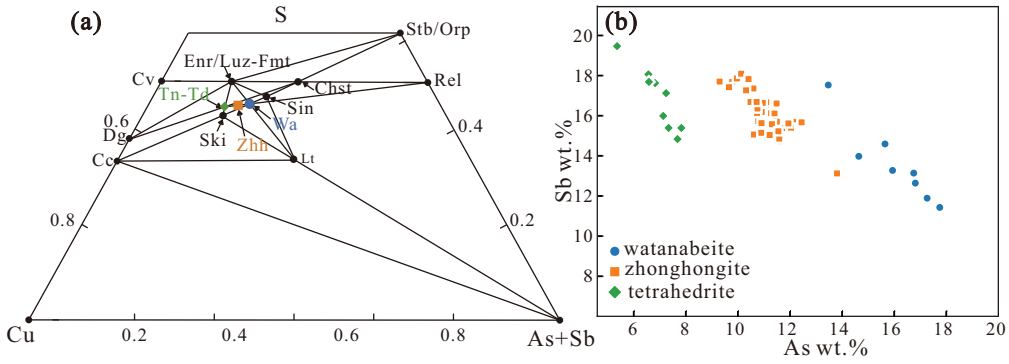

Fig.4

This is the peer-reviewed, final accepted version for American Mineralogist, published by the Mineralogical Society of America.
The published version is subject to change. Cite as Authors (Year) Title. American Mineralogist, in press.
DOI: https://doi.org/10.2138/am-2024-9338. http://www.minsocam.org/

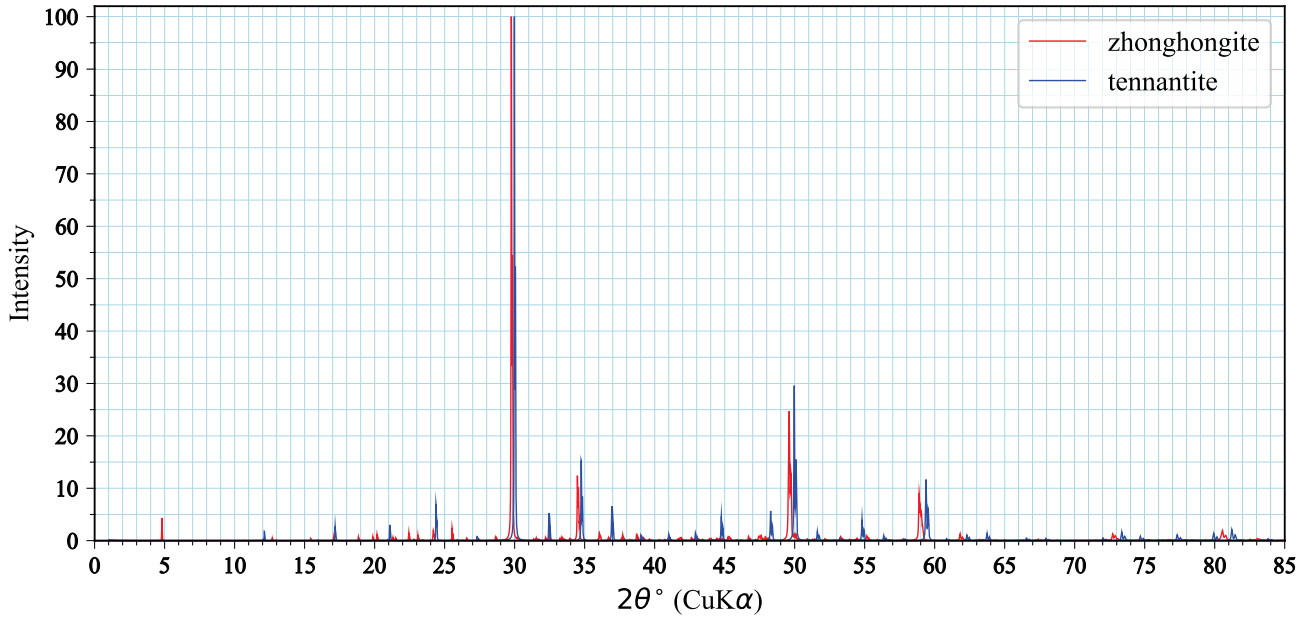

Fig.5

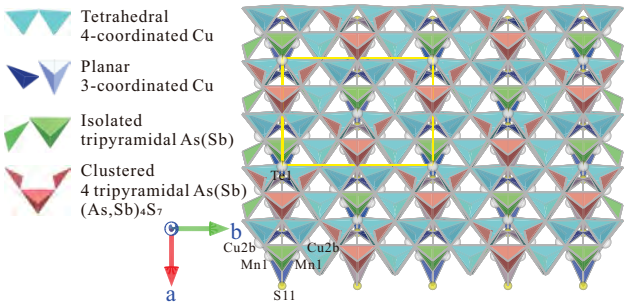

Fig.6

This is the peer-reviewed, final accepted version for American Mineralogist, published by the Mineralogical Society of America.
The published version is subject to change. Cite as Authors (Year) Title. American Mineralogist, in press.
DOI: https://doi.org/10.2138/am-2024-9338. http://www.minsocam.org/

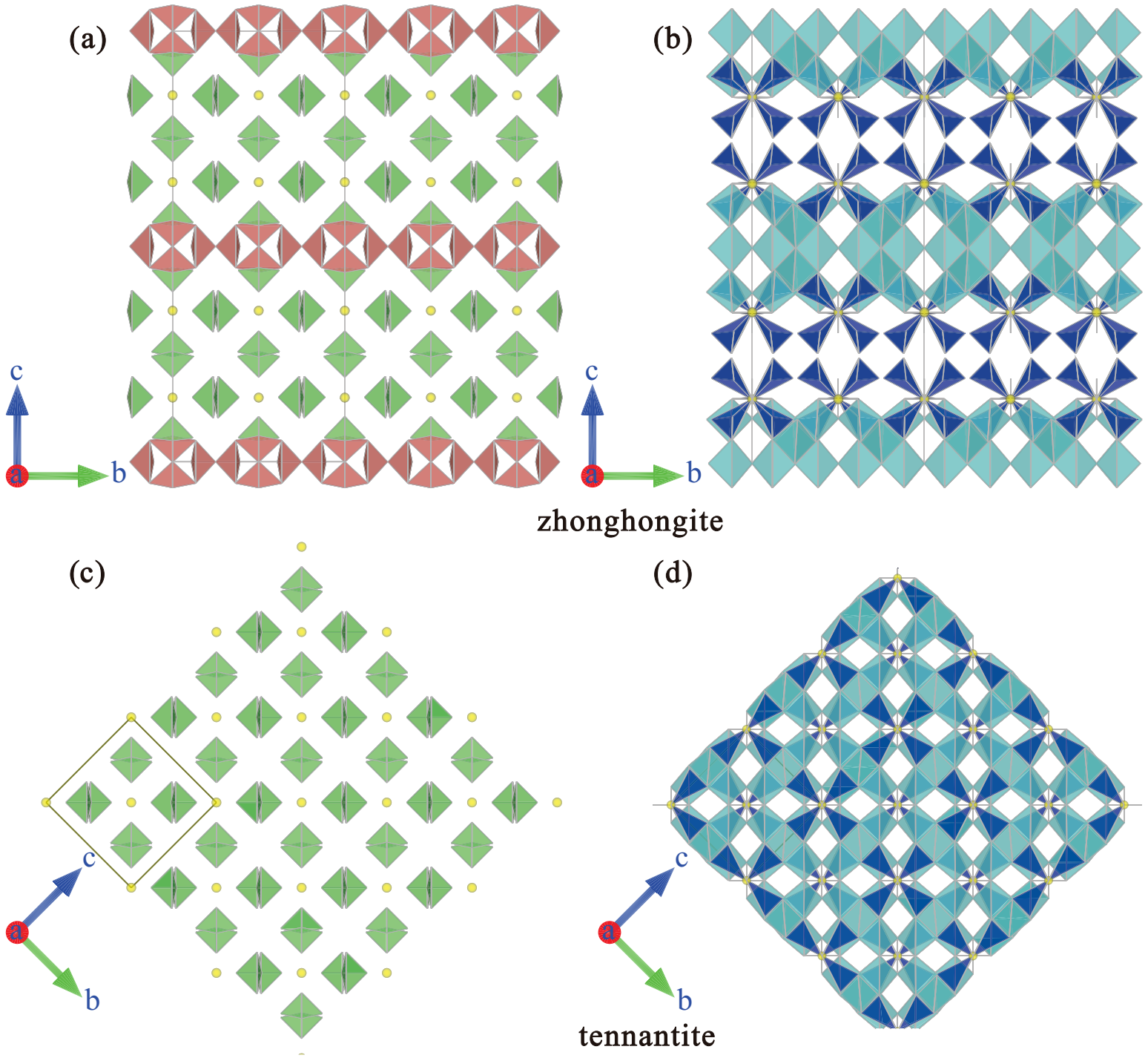

Fig.7